Reviews

Evolution of Red Organic Light-Emitting Diodes: Materials and Devices

Chin-Ti Chen

Institute of Chemistry, Academia Sinica, Taipei, Taiwan 11529

Received February 29, 2004. Revised Manuscript Received April 24, 2004

This short review surveys the development of red fluorescent materials for the application of organic light-emitting diodes (OLEDs) that generate red electroluminescence (EL). The merit and problems of current dopant-based, either fluorescent or phosphorescent, red OLEDs will be addressed first. Materials that offer unique EL characteristics, such as narrow and saturated red EL as well as current density or voltage-independent EL efficiency, are discussed. In addition to dopant-based and assist dopant-based red OLEDs for comparison purposes, the survey emphasizes nondoped red OLEDs that are fabricated with the newly emerging red fluorophores as the host-emitter. The advantage of host-emitting nondoped OLEDs compared with traditional dopant-based red OLEDs is described in view of the chemical and device structures of these materials.

Introduction

Light-emitting materials are the primary substance for organic light-emitting diodes (OLEDs) that generate electroluminescence (EL) in flat panel display applications. Fundamentally, EL originates from electron and hole recombination on fluorescent materials in the thin film layer structure of OLEDs. The light-emitting materials can be in two possible forms, either as the emitter itself (host-emitter) or as the dopant incorporated into an appropiate host. The latter efficiently utilizes the Förster resonance energy transfer from the host. The most frequently used material is the green fluorescent material tris(8-hydroxyquinoline)aluminum (Alq_3). Numerous fluorescent materials, either as host-emitters or dopants, have been known and developed since reports from Kodak on green OLED in 1987 and the dopant-based green and red OLEDs in 1989.[1,2] Whereas short wavelength light-emitting blue or green fluorescent materials are commonly used as either host-emitter or dopant, red fluorescent materials are less flexible and mostly limited to the dopant usage in the fabrication of red OLEDs. This is due to the nature of red fluorescent materials. Fluorophores emitting long enough wavelength (emission maximum wavelength $\lambda_{max} > 610$ nm) are usually polar, such as electron-donor-substituted pyran-containing compounds, or nonpolar but extensively π-conjugated, such as polycyclic aromatic hydrocarbon (PAH) or porphyrin-type macrocyclic compounds. Red emitters used in OLEDs include materials that are highly emissive in solution, such as Nile Red, **DCM** (4-(dicyanomethylene)-2-methyl-6-[4-(dimethylaminostyryl)-4*H*-pyran]), and those more weakly emissive, such as **TPP** (5,10,15,20-teraphenylporphyrin) (Figure 1). However, all these red fluorophores are prone to aggregation in solid state, due to either attractive dipole−dipole interactions or effective intermolecular π-stacking. Therefore, they are highly susceptible to concentration quenching and become either weakly emissive or even not emissive at all in solid state (Figure 1).

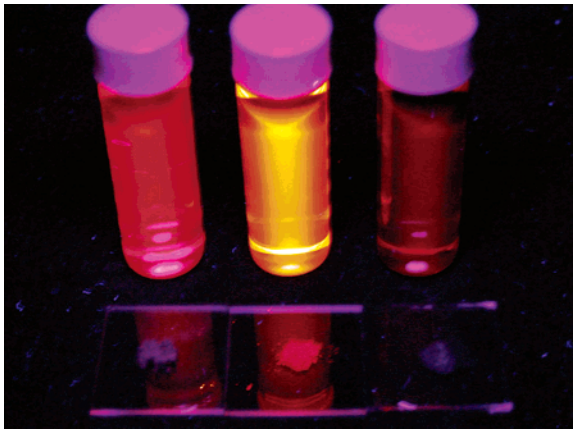

Figure 1. Fluorescence image of Nile red (left), **DCM** (center), and **TPP** (right) in solution (CH_2Cl_2) and in solid state. Please note that the fluorescence of the solid samples of Nile red and TPP is virtually invisible.

Consequently, the guest−host doped emitter system becomes a universal method for solving the problem of these red emissive materials when applied for OLEDs. Dopant molecules are dispersed and isolated in the host materials and thus concentration quenching can be avoided. However, the optimum dopant concentration is usually low, commonly no greater than 2%, and the effective doping range is extremely narrow and commonly no greater than ±0.5% of the optimum concen-

10.1021/cm049679m CCC: $27.50
Published on Web 06/26/2004

Scheme 1

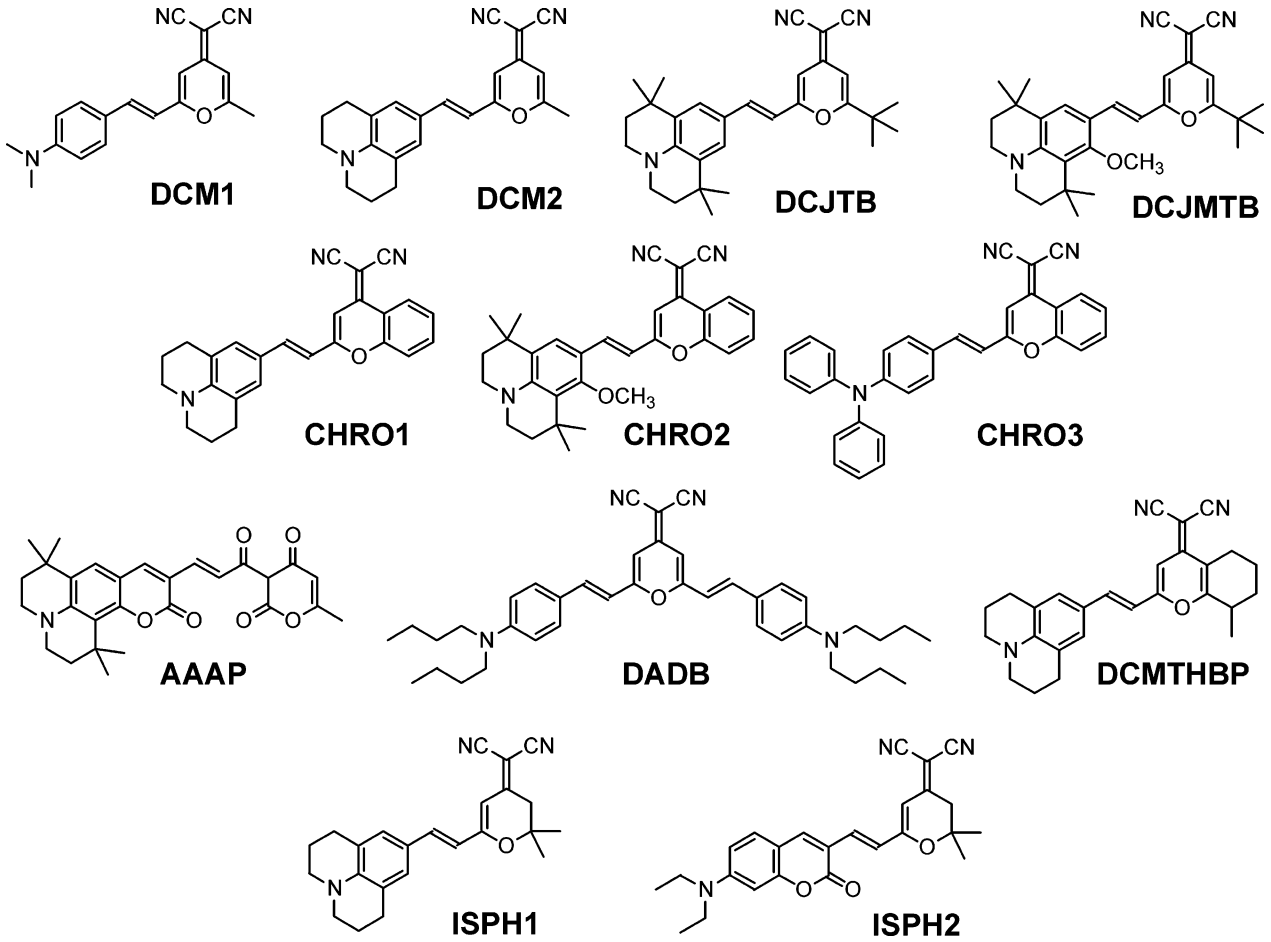

tration.[2] Realistically, OLEDs based on dopant are more difficult to adapt for mass production processes than those based on a nondoped host emitter, considering that reproducibility of the optimum doping level requires careful manufacturing control. From a practical standpoint, a solution to the red-light-emitting OLEDs, either in materials or devices perspective, is highly needed.

This short review will comprehensively survey recently emerging red-light-emitting materials that are used as nondoped host emitters in red OLEDs, which are rare. These materials have attracted growing attention as a possible solution to the problem of red OLEDs.[3] The review is organized first to summarize the current development of red dopant OLEDs, mainly focusing on pyran-containing red dopants, namely **DCM**, **DCM2**, **DCJTB**, **DCJMTB**, and congeners (Scheme 1). A few red dopants other than the **DCM**-type dyes will be mentioned also for their unique EL characteristics, such as stable EL efficiency and narrow emission spectra. To have a fair comparison, we will exclude OLEDs showing red EL with CIE (Commission Internationale de l'Eclairage) 1931 color chromaticity coordinates $x \leq 0.62$ and $y \geq 3.7$ to be accordant or comparable with (0.64, 0.34) and (0.64, 0.33) of the standard red CRT Phosphors of the Society of Motion Picture and Television Engineers (SMPTE-C) and the European Broadcasting Union (EBU), respectively.[4] Except for a handful of examples, reported red OLEDs that do not show the data of color chromaticity coordinates will not be discussed here. Those red OLEDs reported with only an emission maximum of EL (λ_{max}^{EL}) are hard to judge for their color purity of red EL, even though sometimes EL spectra are provided. This review does not cover europium metal complexes, which are known for saturated red emission with extremely narrow full width at half-maximum (fwhm) of only 3 nm.[5] Red OLEDs fabricated with such rare-earth emitters usually fall short of the efficiency and chemical stability required by commercial application, although external quantum efficiency and current efficiency as high as 4.3% and 4.7 cd/A, respectively, have been reported recently.[6] The review also will not cover the very bright and efficient triplet-state red emitters such as iridium complexes or platinum porphyrin complexes.[7] The very good performance of these triplet-state emitters is observed only for the devices operated at relatively low current densities of 0.01−10 mA/cm^2. Emission quenching due to the long lifetime of the triplet state causing severe triplet−triplet annihilation is significant even at medium current density of greater than 50 mA/cm^2 for most cases. Doping is so far compulsorily required for europium metal complexes or triplet-state emitters in practical red OLED application.

Red OLEDs Based on Red Dopant

Although quite a number of red fluorescence dyes have been synthesized and studied, **DCM**-type dyes, particularly **DCJTB**, are still the most efficient materials among them. Both **DCM** and **DCM2** were adopted by Tang et al of Kodak in the classical report demon-

Table 1. EL Performances of Pyran-, Chromene-, or Isophorene-Containing Dopant-Based Red OLEDs

	red dopant	λ_{max}^{el} (nm)	CIE (x, y)	luminance max, at 100 mA/cm^2, at 20 mA/cm^2 (cd/m^2)	maximum efficiency η^{EXT}(%), η^{CR} (cd/A), η^{PW} (lm/W)	reference
1	**DCM2**[a]	650	0.64, 0.36	1400, −, −	−, −, 0.011	8
2	**DCM2**[b]	644	0.64, 0.36	7780, −, −	−, −, −	10
3	**DCJTB**[c]	630	0.64, 0.35	−, −, −	−, 3.24, 1.19	11
4	**DCJTB**[d]	630	0.65, 0.35	−, −, 966	−, 4.44, 2.09	12
5	**DCJMTB**[e]	624	0.63, 0.36	14686, 2500[m], 400[m]	−, 2.64, 0.72	17
6	**AAAP**[f]	630[m]	0.63, 0.36	5600, 1200[m], 300[m]	−, −, −	18
7	**CHRO1**[g]	650[m]	0.63, 0.35	1010, 350[m], 60[m]	−, −, 0.071	19
8	**CHRO2**[h]	660[m]	0.66, 0.33	250, 150[m], 25[m]	−, −, 0.042	19
9	**DADB**[i]	649	0.64, 0.35	−, −, −	−, 0.12, −	20
		653	0.66, 0.34	>250[m], 60[m], 15[m]	−, 0.09, −	
10	**DCMTHBP**[j]	660	0.67, 0.32	414, 390[m], 100[m]	−, 0.29, −	21
11	**ISPH1**[k]	680[m]	0.64,0.33	595, −, −	−, 0.24, 0.08	22a
12	**ISPH2**[l]	670[m]	0.64,0.34	523, −, −	−, 0.16, 0.05	22a

[a] ITO/NPB/Alq_3:**DCM2**(10%)/Mg:Ag. [b] ITO/CuPc/NPB/Alq_3:rubrene(5%):**DCM2**(2%)/Mg:In. [c] ITO/CF_x/NPB/Alq_3:rubrene(5%):**DCJTB**(2%)/Alq_3/LiF/Al. [d] ITO/CF_x/NPB/Alq_3:rubrene(60%):**DCJTB**(2%)/Alq_3/LiF/Al. [e] ITO/TPD/Gaq_3:**DCMJB**(1%)/Gaq_3/Mg:Ag. [f] ITO/TPD/Alq_3:**AAAP**(1.5%)/bOXDF/Alq_3/Mg:Ag. [g] ITO/TPD/Alq_3:**CHRO1**(1%)/Alq_3/Mg:Ag. [h] ITO/TPD/Alq_3:**CHRO2**(1%)/Alq_3/Mg:Ag. [i] ITO/TPD/Alq_3:**DADB**(4.6%)/Alq_3/Al and ITO/TPD/Alq_3:**DADB**(5.2%)/Alq_3/Al. [j] ITO/CuPc/NPD/Alq_3:**DCMTHBP**(2%)/Alq_3/Mg:Ag. [k] ITO/NPB/Alq_3:**ISPH1**(1%)/Alq_3/Mg:Ag. [l] ITO/NPB/Alq_3:**ISPH2**(1%)/Alq_3/Mg:Ag. [m] Estimated from the figures in reference.

Table 2. Red OLEDs, Doped or Non-Doped, Fall Short on the CIE Chromaticity of Standard Red Color

	red emitter	λ_{max}^{el} (nm)	CIE (x, y)	luminance max, at 100mA/cm^2, at 20 mA/cm^2 (cd/m^2)	maximum efficiency η^{EXT}(%), η^{CR} (cd/A), η^{PW} (lm/W)	reference
1	**DCM**[a]	650	0.62, 0.37	150, −, −	−, −, −	9
2	**DCJTB**[b]	620	0.63, 0.37	−, −, 378	−, 1.89, 0.65	13
3	**DCJTB**[c]	620	0.63, 0.37	−, −, 60	−, 5.66, −	16
4	**DCJTB**[d]	628	0.62, 0.38	15000, 6000[l], 1200[l]	−, 3.0, −	15
5	**BSN**[e]	630	0.63, 0.37		−, 2.8, −	3a
6	**D-CN**[f]	597	−, −	5080, 1440, 600[l]	1, −, −	36
7	**D-CN**[g]	598	−, −	3500[l], 3290, 700[l]	1.1, −, −	36
8	**CHRO3**[h]	670[l]	0.63, 0.37	850, 350[l], 50[l]	−, −, 0.059	19
9	**DCDDC**[i]	630	−, −	5600, 1000[l], 200[l]	−, −, 1.6	22b
10	**DADB**[j]	644	0.63, 0.37	>550, 250[l], 60[l]	−, 0.29, −	20
11	**BAM**[k]	620	−, −	6230, 1200[l], 250[l]	−, −, 1.2	40

[a] ITO/TPB/Alq_3:**DCM**(10%)/Mg:Ag. [b] ITO/CF_x/NPB/Alq_3:**DCJTB**(1%)/Alq_3/Mg:Ag. [c] ITO/NPB/Alq_3:**DCJTB**(0.5%)/BCP/Mg:Ag. [d] ITO/NPB/Alq_3:QAD(0.5%):**DCJTB**(1%)/Alq_3/LiF/Al. [e] ITO/2-TNATA/NPB/**BSN**/Alq3/Li_2O/Al. [f] ITO/**D-CN**/Mg:Ag. [g] ITO/**D-CN**/OXD/Mg:Ag. [h] ITO/TPD/Alq_3:**CHRO3**(3%)/Mg:Ag. [i] ITO/PVK:TPD/Alq_3:**DCDDC**(1%)/Mg:Ag. [j] ITO/TPD/Alq_3:**DADB**(3.4%)/Alq_3/Al. [k] ITO/PVK:TPD/Alq_3:**BAM**(1.0%)/Mg. [l] Estimated from the figures in reference.

strating the dopant approach in enhancing the performance of OLEDs.[2] However, the devices they fabricated were not truly red but orange at the optimum doping concentration, which is about 0.1−0.5% for **DCM**, although both provide respectable external quantum efficiency (η^{EXT}) as high as 2.3%. The λ_{max}^{EL} of **DCM** or **DCM2** containing OLEDs is highly concentration-dependent in the ranges of 570−620 and 610−650 nm, respectively (see Figure 2 for **DCM**).

The real red or near-red OLEDs based on **DCM** and **DCM2** were realized later with high doping concentration of 10% (see entry 1 of Table 1 and Table 2).[8,9] However, such red devices showed low brightness and efficiency and thus are unsuitable for practical usage.

To solve the problem of concentration quenching, Hamada et al of Sanyo reported an innovative solution, the so-called "assist dopant" method.[10] Rubrene (5,6,11,12-tetraphenylnaphthacene) was added as codopant with **DCM**-type red emitter in the fabrication of red OLEDs. This is to take advantage of the well-aligned energy level of Alq_3-rubrene-**DCM** fluorophore that facilitates the Förster resonance energy transfer. Rubrene filled in the gap of energy transfer between Alq_3 host and **DCM**-type red dopant, which becomes a problem when the doping concentration is being pushed higher for acceptable color purity of red EL. The assist

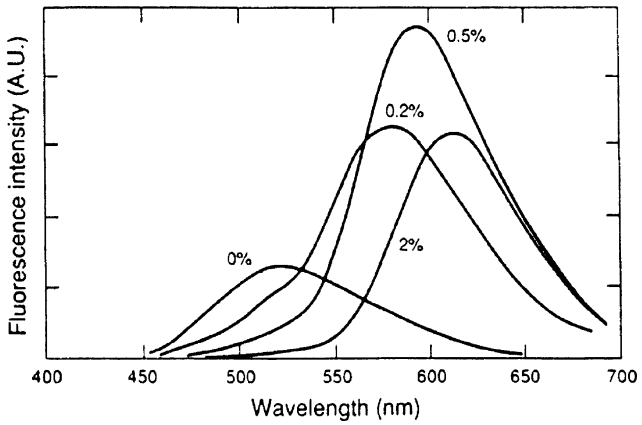

Figure 2. Fluorescence spectra of **Alq_3** doped with **DCM** as a function of **DCM** concentration. (Reprinted with permission from ref 2, Copyright 1989, American Institute of Physics).

dopant approach is quite successful and clearly shows in the **DCJTB**-based red OLEDs when compared to entries 2−4 of Table 1[10−12] with that of non-assist dopant (entry 2 of Table 2).[13] In fact, the assist dopant entry 4 of Table 1 is the red OLED showing the highest EL efficiency (current efficiency η^{CRN} of 4.44 cd/A) among all those listed. Although the information about the maximum EL intensity of the device was lacking, the impressive brightness of 966 cd/m^2 at 20 mA/cm^2

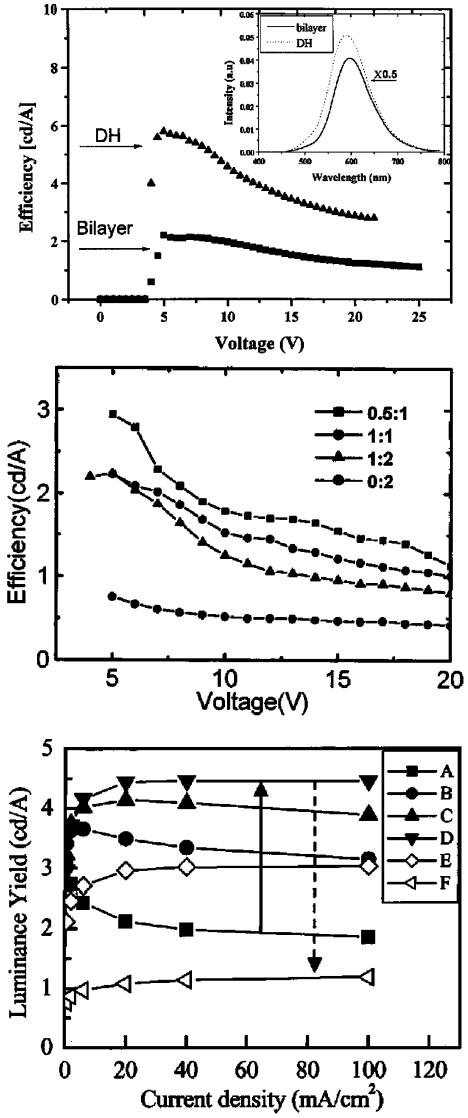

Figure 3. Top: Current efficiency−voltage characteristics (symbols marked with DH) of the device ITO/NPB/Alq_3:**DCJTB**(0.5%)/BCP/Mg:Ag (entry 3 of Table 2). Center: Current efficiency−voltage characteristics (square symbol line) of the device ITO/NPB/Alq_3:QAD(0.5%):**DCJTB**(1%)/Alq_3/LiF/Al (entry 4 of Table 2). Bottom: Current efficiency (luminance yield)−voltage characteristics (solid triangle symbol line) of the device ITO/CF_x/NPB/Alq_3:rubrene(60%):**DCJTB**(2%)/Alq_3/LiF/Al (entry 4 of Table 1). (Reprinted with permission from refs 16, 15, and 12, respectively, Copyright 2001 and 2003, American Institute of Physics).

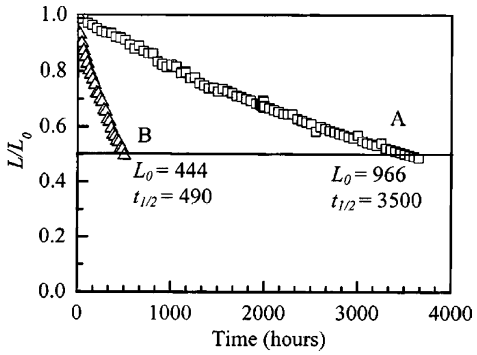

Figure 4. Luminance (L)/initial luminance (L_0) vs time (plot A) of the device ITO/CF_x/NPB/Alq_3:rubrene(60%):**DCJTB**(2%)/Alq_3/LiF/Al (entry 4 of Table 1) driven at 20 mA/cm^2. (Reprinted with permission from ref 12, Copyright 2003, American Institute of Physics).

was mentioned briefly.[12] With the **DCJTB** concentration fixed at 2%, the red OLED showed the best current efficiency (η^{CRN} = 4.44 cd/A) with the concentration of rubrene at 60% and was virtually unaffected by drive current density in the range of 20−100 mA/cm^2.[12] It was suggested that the presence of a large amount of rubrene in the **DCJTB**-doped device can remove excess holes that are injected at high current density and thus reduce the propensity for the formation of cation radical of Alq_3, which was proven for the quenching species can also lead to device instability.[14] The assist dopant quinacridone (QAD) worked similarly to rubrene for red OLED with Alq_3 as the host matrix (entry 4 of Table 2).[15] Lee et al.[16] also enhanced the efficiency of **DCJTB**-doped red OLED to 5.66 cd/A (entry 3 of Table 2) by the addition of a hole-blocking layer of BCP (bathocuproine or 2,9-dimethyl-4,7-diphenyl-1,10-phenanthroline) in the device. The introduction of a BCP layer can confine both charge carriers and excitons in the narrow Alq_3/red dopant recombination zone (only 7 nm). The BCP hole-blocking layer is also important in enhancing the device performance of the nondoped host emitting red OLED (vide infra).

There are a limited number of papers that provide lifetime information of the device, even though it is the major concern for practical application. In most of the OLED studies, the current density or voltage dependency of EL efficiency are shown as an alternative and quick demonstration, although such demonstration does not directly relate to the performance of operation lifetime. Figure 3 illustrates three examples based on the highly efficient **DCJTB**-doped red OLEDs.[12,15,16] The device containing **DCJTB** with rubrene assist dopant exhibited the most stable EL efficiency among the three. Only one of three cases shown in Figure 3 has been tested for the time-dependent performance of the device EL brightness (Figure 4).[12] It was claimed that, assuming the scalable Coulombic degradation, for driving at L_0 of 100 cd/m^2, the half-life ($t_{1/2}$) of this device was projected to be near 3.5 years (>30 000 h).

From a chemical structure standpoint, **DCM2** can be considered an improved version of **DCM**. **DCM2** has a ring-locked alkylamino donor group that increases the molecular rigidity and red-shifts the emission wavelength (about 20−30 nm) which helps in achieving the red EL of the device at lower doping concentration and thus gives better performance (brightness and efficiency) of the device. Red dopant **DCJTB** can be considered as a further improvement of **DCM2**. The molecules of **DCJTB** are built with sterical hindered structural moieties, tetramethyl and *tert*-butyl substituents. Both structural features prevent the **DCJTB** molecules from the close contact that is the origin of concentration quenching. This improvement was clearly shown in the optimum doping concentration of **DCM**/**DCM2** and **DCJTB**, ~0.5% and 2%, respectively. In addition, the *tert*-butyl substituents of **DCJTB** eliminate the reactive methyl group on the pyran ring of **DCM** and **DCM2**, which greatly improves the thermal stability of **DCM**-type red fluorophores and is beneficial for the OLED fabrication.[13] There are many red fluorophores derived from **DCM**-type molecules, such as

Table 3. EL Performances of Dopant Red OLEDs with Either Saturated Red Emission (1−7) or Stable Efficiency over a Wide Range of Current Densities (8 and 9)

	red host-emitter	λ_{max}^{el} (nm)	fwhm (nm)	CIE (x, y)	luminance max, at 100 mA/cm^2, at 20 mA/cm^2 (cd/m^2)	maximum efficiency η^{EXT}(%), η^{CR} (cd/A), η^{PW} (lm/W)	reference
1	**TPP**[a]	655	25[j]	0.70, 0.28	42, 30[j], 10[j]	0.07, −, −	23
2	**TPC**[b]	660	20	0.67, 0.29	100, −, −	−, −, 0.061	24
3	**TPDPP**[c]	635	25[j]	0.69, 0.29	150, −, −	−, −, 0.035	25
4	**ACY**[d]		68	0.68, 0.32	6400, −, −	0.8, −, 1.3	26
5	**CQY**[e]		60	0.70, 0.30	1000, −, −	0.12, −,0.28	26
6	**BDPMB**[f]	640[j]	65	0.67, 0.33	2880, −, 285	−, 1.34, −	27
7	**BDPMBZn**[g]	640[j]	75[j]	0.66, 0.33	2260, −, 125	−, 0.46, −	27
8	**DPP**[h]	625		0.63, 0.34	1500[j], 150[j], 20[j]	−, 1.2, 0.33	31
9	**pAAA**[i]	616		0.63, 0.36	−, −, −	−, 0.6, −	32

[a] ITO/TPD/Alq$_3$:**TPP**(3%)/Mg:Ag. [b] ITO/TPD/Alq$_3$:**TPC**(1.5%)/Mg:Ag. [c] ITO/NPB/DNA:**TPDP**P(5%)/Alq$_3$/Mg:Ag. [d] ITO/*m*-MTDATA/Alq$_3$:**ACY**(1%)/Mg:Ag. [e] ITO/*m*-MTDATA/Alq$_3$:**CQY**(2.2%)/Mg:Ag. [f] ITO/TPD/TPD:BDPMB(1%)/Alq$_3$: **BDPMB**(1%)/Alq$_3$/ Mg:Ag. [g] ITO/TPD/TPD:BDPMBZn(1%)/Alq$_3$:**BDPMBZn**(1%)/Alq$_3$/Mg:Ag. [h] ITP/TPD/Alq$_3$:**DPP**(0.55%)/Alq$_3$/Mg:Ag. [i] ITO/NPB/Alq$_3$:**pAAA**(2%)/Alq$_3$/Mg:Ag. [j] Estimated from the figures in reference.

Scheme 2

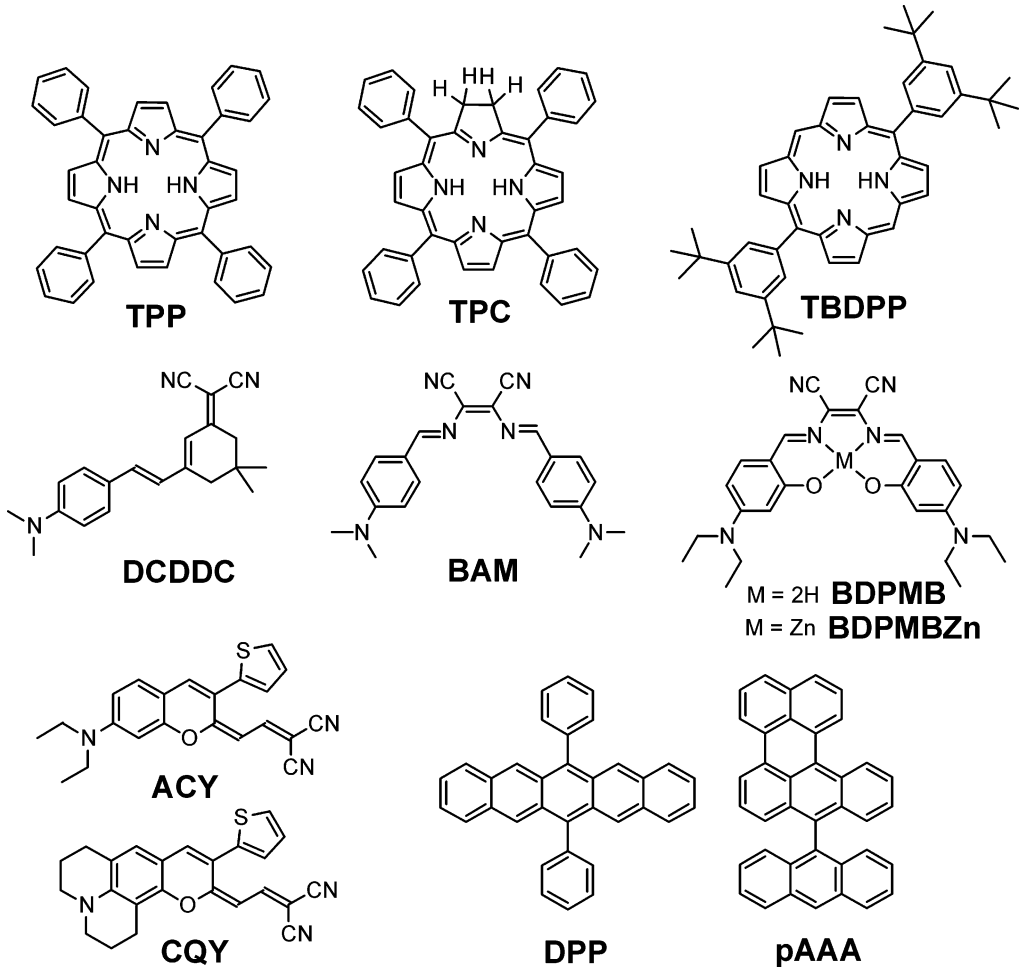

DCJMTB,[17] **AAAP**,[18] **CHRO1**,[19] **CHRO2**,[19] **DADB**,[20] **DCMTHBP**,[21] **ISPH1**,[22a] **ISPH2**[22a] (entries 6−12 of Table 1), or even **CHRO3**,[19] **DCDDC**,[22b] and **DADB**[20] (entries 8−10 of Table 2) which are not so red to the standard of CIE chromaticity. However, all these fluorophores showed performance inferior to that of **DCJTB** when applied for red OLEDs.

Dopant-Based Red OLEDs with Unusual EL Characteristics

One type of unusual red OLED is the EL spectra showing relatively narrow FWFM, usually less than 70 nm. Entries 1−6 of Table 3 are devices of this type containing red dopants **TPP**,[23] **TPC**,[24] **TRDPP**,[25] **ACY**,[26] **CQY**,[26] **BDPMB**,[27] and **BDPMBZn**,[27] respectively (Scheme 2). Among them, macrocyclic compounds, such as **TPP**, **TPC**, and **TPDPP**, show extreme fwhm of EL as narrow as 20 nm (Figure 5). In addition to the narrow fwhm, these macrocyclic compounds also exhibit relatively long wavelength of λ_{max}^{el} in the range of 635−660 nm. Therefore, the red EL of this kind always has saturated red color chromaticity and they are "redder" than the high standard red of NTSC.[4b] They usually appear at the edge of CIE chromaticity diagram and very close to the corner position of standard red.

Table 4. EL Performances of Non-Doped (Host-Emitting) Red OLEDs

		λ_{max}^{el} (nm)	CIE (x, y)	luminance max, at 100 mA/cm^2, at 20 mA/cm^2 (cd/m^2)	maximum efficiency η^{EXT}(%), η^{CR} (cd/A), η^{PW} (lm/W)	reference
1	**(PPA)(PSA)Pe**[a]	579	0.64, 0.35	4800, −, −	−, 1.1, −	33
2	**DCDDC**[b]	650	−, −	30, 3[p], 0.5[p]	−, −, −	22
3	**DCJMTB**[c]	648	0.67, 0.33	1662, 380[p], 130[p]	−, 0.41, 0.12	17
4	**BDCM**[d]	640	0.63, 0.36	582, 100[p], 20[p]	−, −, 0.059	47
5	**TPZ**[e]		0.65,0.33	1766, 324, 69	0.5, 0.34, 0.17	41
6	**NPAMLMe**[f]	650	0.66, 0.32	8000, 1260, 300	2.4, 1.5, 0.9	42
7	**NPAFN**[g]	636	0.64, 0.33	9359, 1800, 455	2.4, 2.5, 1.7	37
8	**NPAFN**[h]	634	0.64, 0.33	10034,1700, 392	1.8, 2.0, 0.9	37
9	**INDMLMe**[i]	650	0.63, 0.36	1750, −, −	0.45[p], −, −	43
10	**ACEN1**[j]	624	0.64, 0.34	5436, 492, −	0.46,0.50, 0.26	34
		624	0.63, 0.34	4451, 503, −	0.48,0.53, 0.33	
		626	0.65, 0.35	4514, 516, −	0.49,0.52, 0.23	
11	**ACEN2**[k]	624	0.64, 0.34	4416, 360, −	0.39, 0.42, 018	34
		622	0.64, 0.34	5225, 561, −	0.51, 0.57, 0.38	
		624	0.65, 0.35	4643, 604, −	0.68, 0.77, 0.60	
12	**ACEN3**[l]	630	0.65, 0.34	2705, 299, −	0.33, 0.31, 0.27	34
13	**ACEN4**[m]	630	0.64, 0.32	1528, 283, −	0.40, 0.28, 0.12	34
		628	0.64, 0.33	1534, 309, −	0.36, 0.33, 0.30	
		626	0.66, 0.34	1764, 350, −	0.37, 0.36, 0.17	
14	**BZTA1**[n]	640	0.63, 0.35	8087, 869, −	0.99, 0.91, 0.58	38
		640	0.65, 0.35	5083, 378, −	0.52, 0.48, 0.30	
15	**BZTA2**[o]	626	0.63, 0.35	9138, 1415, −	1.7, 2.0, 1.6	38
		626	0.64, 0.36	7952, 597, −	0.51, 0.60, 0.44	

[a] ITO/starburst amine/**PPAPSAPe**/quinoline metal complex/Mg:Ag. [b] ITO/PVK:TPD/**DCDDC**/Mg:Ag. [c] ITO/TPD/**DCJMTB**/Alq$_3$/Mg:Ag. [d] ITO/CuPc/DPPhP/**BDCM**/Mg:Mg. [e] ITO/**TPZ**/TPBI/Mg:Ag. [f] ITO/**NPAMLMe**/BCP/TPBI/Mg:Ag. [g] ITO/**NPAFN**/BCP/TPBI. [h] ITO/NPB/**NPAFN**/BCP/TPBI/Mg:Ag. [i] ITO/NPB/**INDMLMe**/TPBI/Mg:Ag. [j] ITO/**ACEN1**/TPBI/Mg:Ag, ITO/NPB/**ACEN1**/TPBI/Mg:Ag, and ITO/NPB/**ACEN1**/BCP/Alq$_3$/Mg:Ag. [k] ITO/**ACEN2**/TPBI/Mg:Ag, ITO/NPB/**ACEN2**/TPBI/Mg:Ag, ITO/NPB/**ACEN2**/BCP/Alq$_3$/Mg:Ag. [l] ITO/NPB/**ACEN3**/BCP/Alq$_3$/Mg:Ag. [m] ITO/**ACEN4**/TPBI/Mg:Ag, ITO/NPB/**ACEN4**/TPBI/Mg:Ag, and ITO/NPB/**ACEN4**/BCP/Alq$_3$/Mg:Ag. [n] ITO/**BTZA1**/TPBI/Mg:Ag and ITO/**BTZA1**/Mg:Ag. [o] ITO/**BTZA2**/TPBI/Mg:Ag and ITO/**BTZA2**/Mg:Ag. [p] Estimated from the figures in reference.

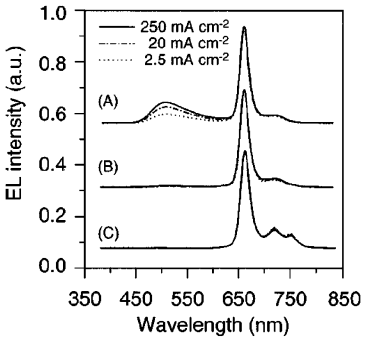

Figure 5. EL spectra of the device ITO/TPD/Alq$_3$:**TPC**(x%)/Mg:Ag, $x = 0.5$% (A), $x = 1.7$% (B), and $x = 3.7$% (C). (Reprinted with permission from ref 24, Copyright 1999, American Institute of Physics).

Although their red OLEDs have not been satisfactory in brightness and efficiency, porphyrin-type macrocyclic red dopants having such long emissive wavelength and narrow EL are quite special and few other materials show comparable properties. Squarylium dyes probably are the few exceptional cases. Squarylium compounds are also well recognized for their long emission wavelengths (usually 640−700 nm) and narrow emission spectra (fwhm 20−50 nm) in solution, although concentration quenching is as severe as that with porphyrin-type macrocyclic compounds. However, one adverse property of squarylium dyes is their very small Stokes shifts of only about 10−20 nm. This hampers them from being used for red OLEDs even in dopant form. Most of the red fluorescent squarylium dyes absorbed in relatively long wavelength (620−670 nm), which makes them very inefficient in the Förster resonance energy transfer from the green emissive host such as Alq$_3$ that emits light around 530 nm. There was always nominal, but not negligible, green emission in the red OLEDs doped with squarylium dye. Therefore, red OLEDs with squarylium dopant have never provided pure red EL so far.[28−30] Because of the very close absorption and emission energies, self-absorption of EL from squarylium red dopant is significant and thus greatly reduces the intensity and efficiency of the device.

In most cases, the EL efficiency of red OLEDs starts to decay at elevated current densities or driving voltages, regardless of whether EL originates from fluorescence or phosphorescence. This is almost a universal phenomenon, found in both dopant-based red OLEDs and nondoped red OLEDs. A couple of cases, **DPP** and **pAAA** (entries 8 and 9 of Table 3, respectively), are exceptional.[31,32] Red OLEDs based on these two red dopants show unchanged EL efficiency over a wide range of current densities—as high as several hundred mA/cm^2 (see Figure 6 for example). As far as chemical structure, unlike most other red fluorophores containing heteroatoms, often nitrogen and oxygen, these two fluorophores are classical PAH-type compounds that have only carbon and hydrogen as the composing elements. Unfortunately, even though they have impressive efficiency stability, red OLEDs containing PAH-type red dopant do not meet the requirement of EL intensity (either maximum or at low current density) and efficiency (entries 8 and 9 of Table 3).

Host-Emitting Nondoped Red OLEDs

The first reported host-emitting nondoped red OLED was by Toguchi et al of NEC (entry 1 of Table 4).[33] The red host emitter is **(PPA)(PSA)Pe**, which is a styryl-appended diarylamine derivative of a perylene compound, also a PAH moiety (Scheme 3). **(PPA)(PSA)Pe** has a rather short emission λ_{max} of 579 nm. Normally, such a short emission wavelength will not provide

Scheme 3

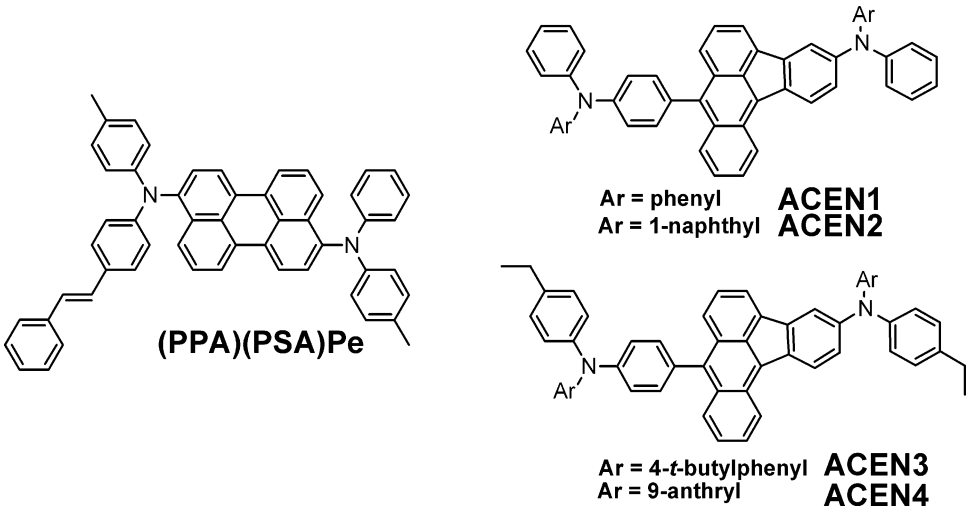

sufficient red EL for OLEDs. The device still showed satisfactory red color chromaticity (CIE coordinates $x = 0.64$, $y = 0.35$) because of the shoulder band at longer wavelength of 620 nm of the EL spectra that was attributed to the eximer emission. Excimer formation is usually an indication of the tendency of the materials to aggregate or crystallize.

More recently, Lin et al.[34] also have reported a series of diarylamine-encapsulated benzo[*a*]aceanthrylene compounds **ACEN**s, also a PAH-type species for nondoped red OLEDs (entries 10−13 of Table 4). These **ACEN** compounds provided long enough emission wavelengths and thus most OLEDs fabricated with **ACEN** were sufficiently red. Furthermore, **ACEN3** and **ACEN4** were reported to be amorphous materials based on the lack of detectable melting temperature in the differential scanning calorimetry (DSC) measurements. Nevertheless, nondoped red OLEDs made from these arylamine-substituted PAH compounds were neither bright nor efficient. This can be partially attributed to the low solution fluorescence quantum yield (ϕ^f) of the **ACEN** compounds (ϕ^f 5−12%).[34] Molecules of **ACEN**s (as well as **(PPA)(PSA)Pe**) were built with triarylamine moieties, which have been demonstrated to enhance the amorphous property and thus solid-state fluorescence intensity.[35] However, the hole-transporting nature of theses red **ACEN** compounds (basically they are hole-transporting triarylamine species) renders the OLEDs loss balance on the charge carriers of hole and electron. A wide band-gap electron-transporting material TPBI (2,2′,2″-(1,3,5-phenylene)-tris-(1-phenyl-1H-benzimidazole) or a hole-blocking material BCP was required for an OLED to generate pure red EL at a minimally acceptable efficiency.

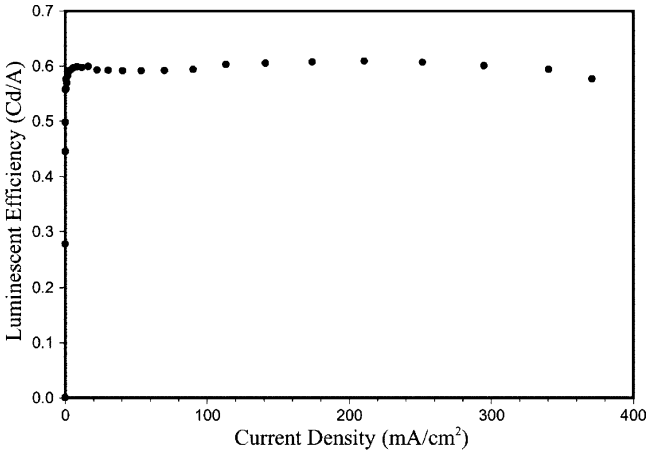

Figure 6. Luminance efficiency of a device with the configuration ITO/NPB/Alq_3:**pAAA**(2%)/Alq_3/Mg:Ag. (Reprinted with permission from ref 32, Copyright 2002, Royal Society of Chemistry).

The second type of nondoping red material for OLED can be classified as donor−acceptor-substituted fluorophores. Normally, this type of fluorophore is highly polar and thus vulnerable to aggregation in solid state. However, molecules such as **BSN**,[3a] **D-CN**,[36] **NPAFN**,[37] and **BZTA2**[38] (Scheme 4) possess a pair of antiparallel dipoles, thus fluorescence concentration quenching in solid state due to dipole−dipole interaction can be substantially suppressed. In this regard, **BAM**[40](entry 11 of Table 2) also belongs to the class of material that has not yet been examined for nondoped red OLED. Dipolar red fluorophores seem to offer much better performance than those of arylamine substituted PAHs. First, the existence of both electron donor and acceptor can intensify charge-transfer absorption and the corresponding emission intensity. Second, the hole and electron carriers of the materials can be nearly balanced due to the electron acceptor in addition to the arylamino donor. Devices based on **NPAFN** (entries 7 and 8 of Table 4) and **BZTA2** (entry 15 of Table 4) exhibited two of the brightest nondoped red OLEDs with maximum EL intensities of 10 034 and 9134 cd/m^2, respectively. Here we exclude **BSN** (entry 5 of Table 2) and **D-CN** (entries 6 and 7 of Table 2), because of the lack of the information on EL intensity and color chromaticity, respectively. Pratically, at low current density of 20 mA/cm^2, **NPAFN** showed remarkable EL intensity of 455 cd/m^2 (Figure 7), which was sufficiently bright for flat panel display application. **BZTA2** was weaker, with EL intensity of 1413 cd/m^2 at 100 mA/cm^2 but no data of EL intensity were available at 20 mA/cm^2. Although all decayed at high current densities, in the medium range of current densities of 20−100 mA/cm^2 (or driving voltage of 5−9 V), the EL efficiency of red OLED containing **NPAFN** was about as stable as those of red OLEDs containing **DCJTB** dopant, but inferior to those with

Scheme 4

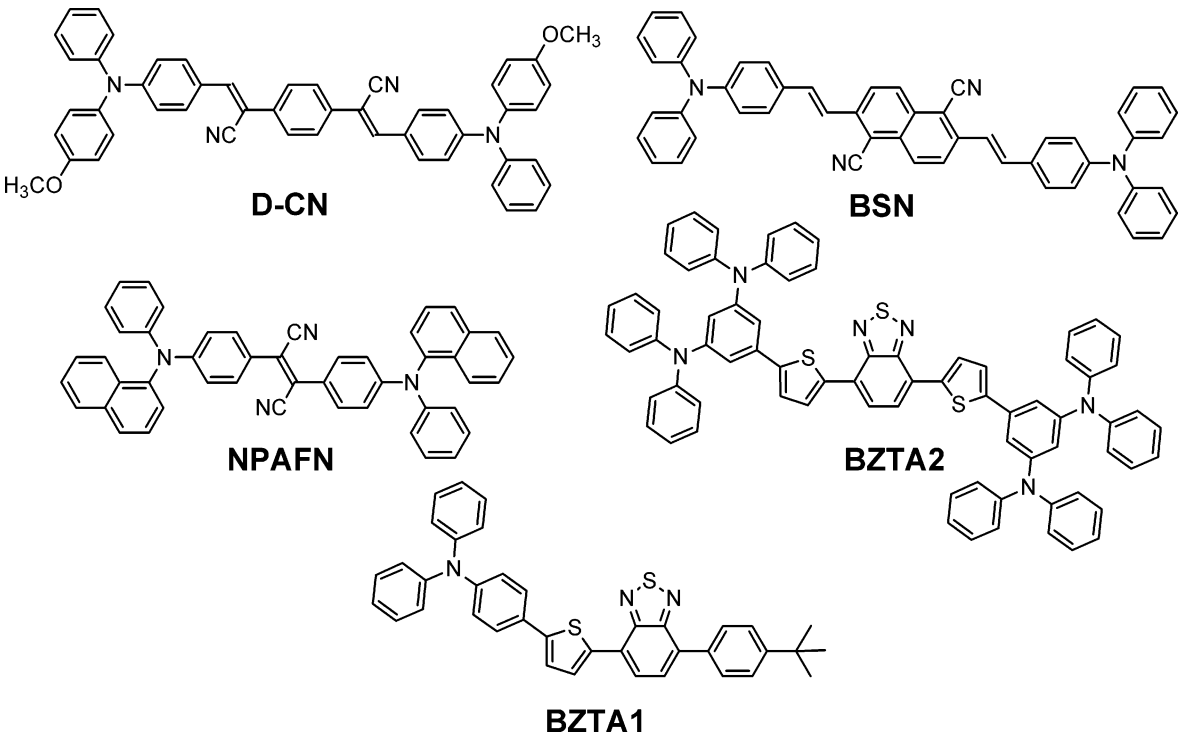

Scheme 5

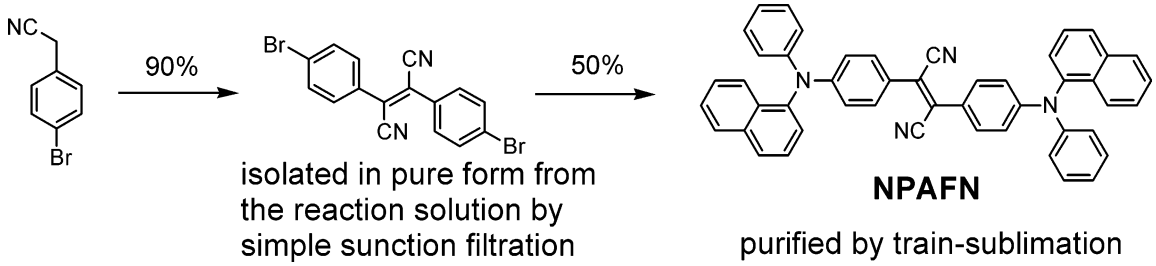

DCJTB dopant and rubrene assist dopant (Figure 3).

The unusual fluorescence of **NPAFN** has also drawn attention.[36] It is unusual because its fluorescence in solid state is much brighter than that in solution (see Figure 8). This is in sharp contrast to other red fluorophores such as Nile Red, **DCM**, or **TPP**, which are susceptible to fluorescence quenching (see Figure 1). Once again, the bulky and nonplanar arylamino substituents were believed to play an important role in preventing the fluorescence of **NPAFN** from quenching in solid state. **NPAFN** was reported to behave as a semi-amorphous material when examined by repeated scans of DSC. It is also worthy of mention that the synthesis of **NPAFN** is quite simple, as it can be

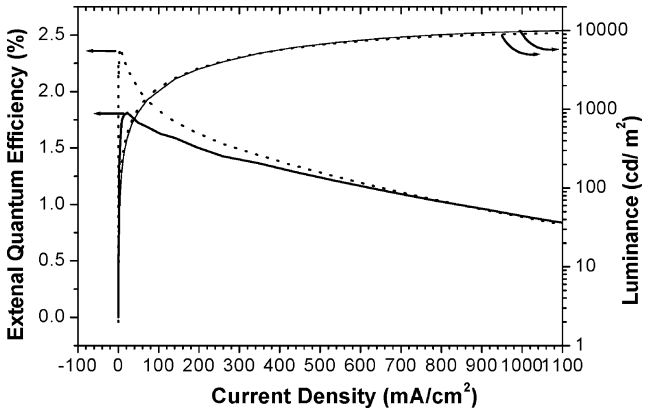

Figure 7. EL intensity and external quantum efficiency of OLED, ITO/NPB(40 nm)/**NPAFN**(30 nm)/BCP(10 nm)/TPBI(30 nm)/Mg:Ag (solid lines) and ITO/**NPAFN**(50 nm)/BCP(10 nm)/TPBI (30 nm)/Mg:Ag (dotted lines). (Reprinted with permission from ref 37, Copyright 2003, Royal Society of Chemistry).

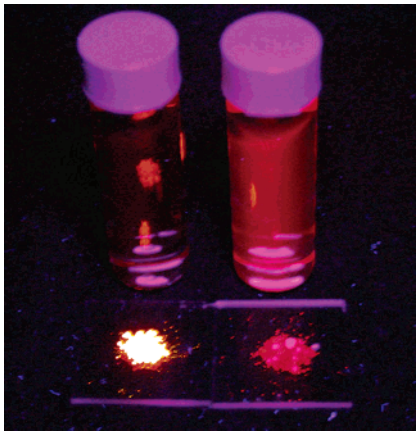

Figure 8. Fluorescence image of **NPAFN** (left) and **NPAMLMe** (right) in solution (CH_2Cl_2) and in solid state. Note that the fluorescence of **NPAFN** in solution can be barely seen.

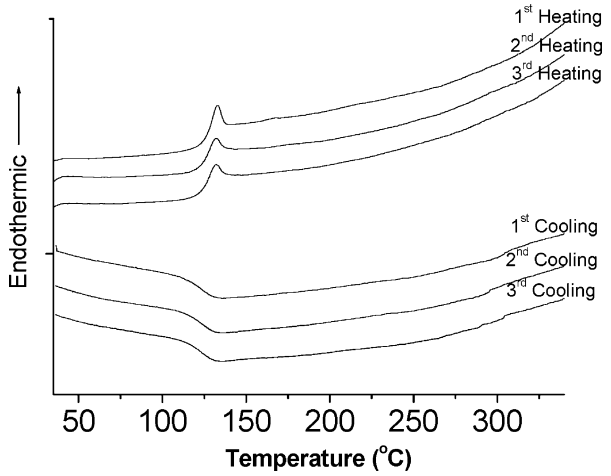

Figure 9. DSC thermograms of **NPAMLMe** with sequential heating and cooling. (Reprinted with permission from ref 42, Copyright 2002, VCH Verlag).

prepared in only two reaction steps with high yields and without involving column chromatography in purification (Scheme 5),[37] compared with that of **DCJTB** which has to be synthesized in multiple reaction steps.[13,39] This makes **NPAFN** quite attractive as a practical material for host-emitting nondoped red OLEDs.

The third type of nondoping red fluorescent material is similar to the second one but differs in the alignment of the intramolecular dipoles. Two reports relevant to the same type of material appeared in the literature within a short period of time by Lin et al.[41] and Chen et al.[42] They reported **TPZ** and **NPAMLMe** independently for the usage of nondoped red OLEDs. Both **TPZ** and **NPAMLMe** adopt a pair of vicinal triarylamine substituents as the electron-donor of the red fluorophore Scheme 6). Two red fluorophores used heterocyclic moiety, thienopyrazine of **TPZ** and maleimide of **NPAMLMe**, as the electron-acceptor. Moderate to strong positive solvatochromism was observed for both **TPZ** and **NPAMLMe**, indicating the dipolar nature of the molecule. Interestingly, whereas both melting and crystallization were detected for **TPZ**, **NPAMLMe** was reported to be a truly amorphous molecular material by showing no detectable melting or crystallization signal but only glass transition temperature signals in all repeating scans of DSC (Figure 9). The amorphous nature of **NPAMLMe** was further confirmed by the broad diffraction signal of power X-ray diffraction spectrum (Figure 10).

Recently, single-crystal structure was obtained for a couple of bisindole-substituted maleimide derivatives, including **INDMLMe** (entry 9 of Table 4).[43] The nonplanar conformation of these maleimide molecules was identified. Furthermore, the implication of polymorphism and hence the possible amorphous tendency of these compounds was obtained by DSC and reflected by the different geometry of the two indole rings that were believed to be easily convertible. Similar to that of **NPAFN**, **NPAMLMe** exhibits very strong red fluorescence in solid state but not in solution (Figure 8). Regarding device performance (entry 5 of Table 4 for **TPZ** and entry 6 of Table 4 for **NPAMLMe**), the OLED containing **NPAMLMe** was much better than that containing **TPZ** in all aspects. On the other hand, although **NPAMLMe** is better with regard to amorphous property, **NPAFN** is clearly a stronger emitter in solid state (Figure 8). Recent measurement of the fluorescence quantum yield of **NPAMLMe** and **NPAFN** in solid state has revealed that **NPAFN** is about twice as bright as **NPAMLMe**.

In fact, before **TPZ** and **NPAMLMe**, in addition to the precedent **(PPA)(PSA)Pe**, **BSN**, and **D-CN**, there were related materials known in the literature, although they were not intentionally designed to be suitable for host-emitting nondoped red OLEDs. They are **PERYN**, **DDCD** (entry 4 of Table 4), **DCMJTB**, **d-DCM**, and **TACN** (Scheme 7). Except for **DCMJTB** (entry 5 of Table 4), their performances as red OLEDs were either far from satisfactory (**DDCD**) or there was a lack of complete characterization data for evaluation, such as **PERYN** (λ_{max}^{el} ~615 nm with fwhm of 77 nm,

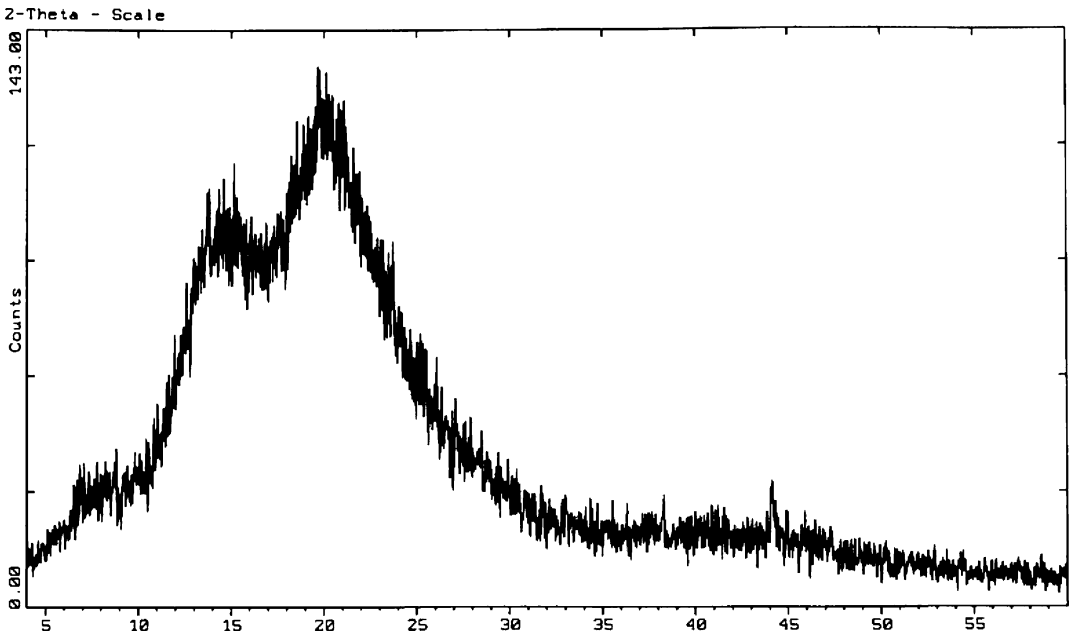

Figure 10. Powder X-ray diffraction spectrum of **NPAMLMe**.

Scheme 6

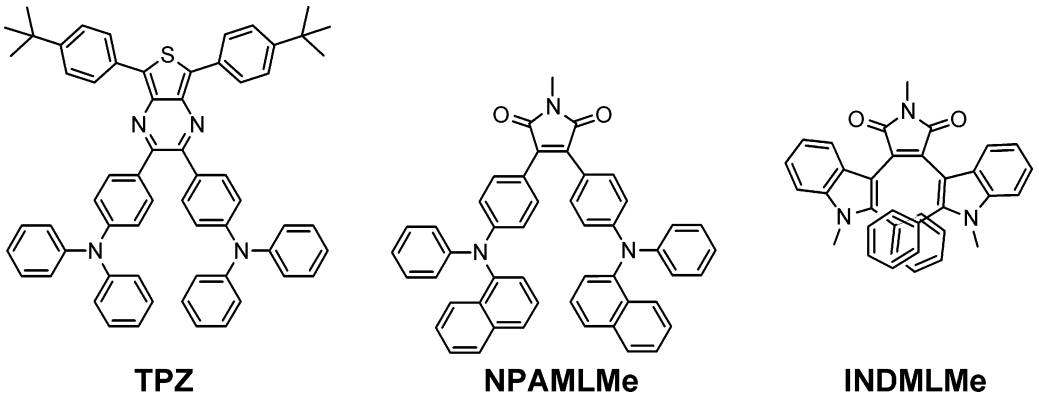

Scheme 7

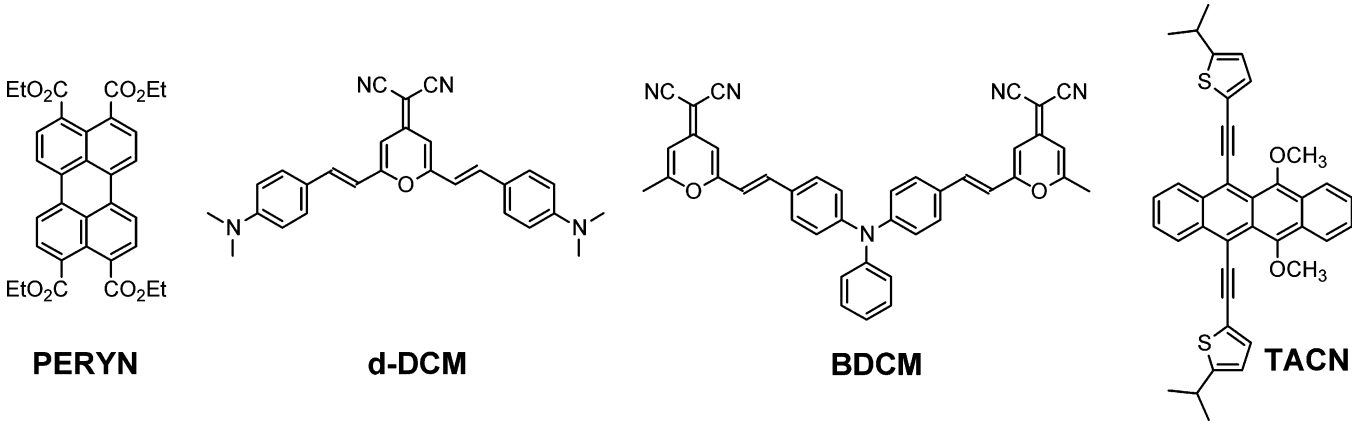

maximum electroluminance 45 cd/m^2 at 28 V),[44] **d-DCM** (λ_{max}^{el} ~610 nm with fwhm of 71 nm with CIE coordinates of (0.65, 0.31)),[45] and **TACN** (λ_{max}^{el} ~656 nm).[46]

One more report by Zhang et al.[47] on **BDCM** appeared just about the same time as the reports on **TPZ** and **NPAMLMe**. **BDCM** is in fact a dimer version of **DCM**. The amorphous property or solid-state fluorescence have not been known for **BDCM** but the host-emitting nondoped red OLED was fabricated with **BDCM**, although the performance was not good enough to be of interest (entry 4 of Table 4). Nevertheless, one thing valuable disclosed by Zhang et al was that the CIE coordinates of the device are nearly unchanged with increasing current density (Figure 11).

Therefore, this is another advantage for host-emitting nondoped red OLEDs offering better device operation compared to red OLEDs with dopants for which the color changes with increasing driving voltages.[48] Similar voltage or current density dependence of EL color was also observed in the emitting assist dopant-based red OLEDs.[10]

More recently, Chen et al. have reported a detailed study on a series of red OLEDs, either with **NPAMLMe** as red dopant or as nondoped host emitter.[49] Their report also showed that the EL of the device is stable with respect to driving voltage. The profile of EL spectra (so the color chromaticity of EL) of the device was virtually unchanged in the range of 8−16 V (Figure 12).

Chen et al. also clearly demonstrated that the thickness of hole-blocking layer of BCP for the nondoped host-emitting red OLEDs was critical. BCP is crucial

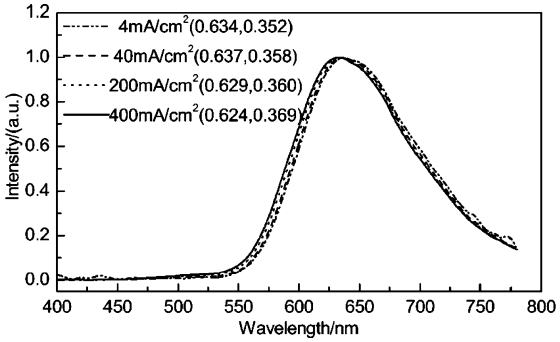

Figure 11. EL spectra of **BDCM** at different current densities. (Reprinted with permission from ref 47, Copyright 2002, The Royal Society of Chemistry).

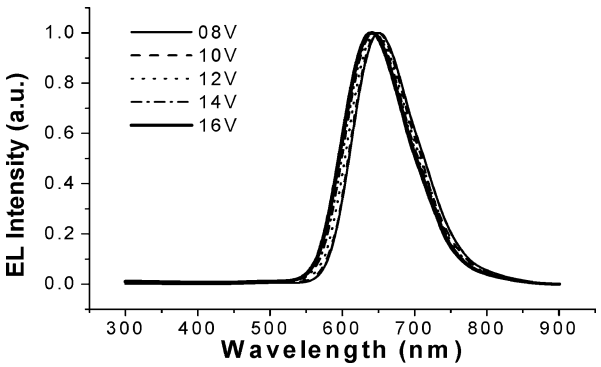

Figure 12. EL spectra (normalized) of device ITO/NPB(5 nm)/**NPAMLMe**(30 nm)/BCP(20 nm)/Alq_3(40 nm)/Mg:Ag at different driving voltages, (Reprinted with permission from ref 49, Copyright 2004, The Royal Society of Chemistry).

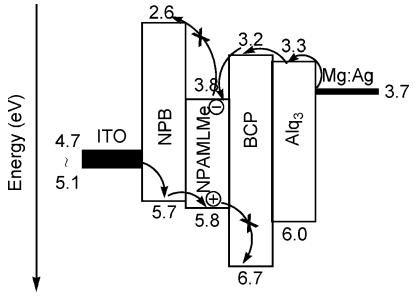

Figure 13. Relative energy diagram of the materials ITO, NPB, **NPAMLMe**, BCP, Alq_3, and Mg:Ag. (Reprinted with permission from ref 49, Copyright 2004, The Royal Society of Chemistry).

for confining the charge-recombination in the emitting layer of **NPAMLMe** and preventing undesired green emission from Alq_3.[50] This is due to the large gap between the HOMO of **NPAMLMe** and BCP as well as between the LUMO of **NPAMLMe** and NPB (bis(4-(*N*-(1-naphthyl)-*N*-phenylamino)phenyl)biphenyl), the hole-transporting material of the device (Figure 13).

Similar function of BCP has been widely utilized in phosphorescence-based OLEDs.[7,51] The performance of the device, turn-on voltage, operating current density, brightness, color purity, efficiency, and even the stability, are highly dependent on BCP.[49,52]

Conclusions

The development of materials for red OLEDs has gone through several important evolutional stages. The red emitters first entered the evolution process as the ingenious dopant and **DCJTB** has been the best material so far. However, very soon people realized the dilemma faced with dopant-based red OLEDs. Basically, efficient and bright dopants are not red enough, and red enough dopants are not efficient and bright. Then there was the invention of the assist dopant approach which resolved the problem associated with concentration quenching red dopant and further enhanced the performance of **DCJTB**-based red OLEDs. Highly efficient and bright phosphorescence-based red OLEDs emerged quickly after, although concentration quenching was more severe than ever and doping was a compulsory approach as a remedy method. More recently, the hard-to-control doping process has been a serious concerned beyond laboratory manipulations, in the practical process of mass production. The latest evolution is the host-emitting nondoped red OLED which avoids the doping process. The success of the evolution hinges on the red fluorophores that are judiciously designed for showing amorphous or semi-amorphous properties and thus diminished concentration quenching. **NPAMLMe**, **NPAFN**, and **BZTA2** are currently the most satisfactory materials to meet this purpose. Among them, **NPAFN** has the advantage of easy synthesis and purification. The current performance of host-emitting nondoped red OLEDs still falls below that of dopant-based red OLEDs, but the lagging distance is closing up as their evolution progresses.

Acknowledgment. I am grateful to the efforts of my colleagues at Academia Sinica, Dr. Hsiu-Chih Yeh, Mr. Li-Hsin Chan, Mrs. Wei-Ching Wu, and Mr. Shi-Jay Yeh, whose work I have cited. The instruction on fabrication and EL characterization of OLEDs from Dr. Yu-Tai Tao is acknowledged. I also thank Mr. De-Chang Dai and Dr. Juen-Kai Wang for their assistance in the determination of the fluorescence quantum yields of **NPAMLMe** and **NPAFN** in solid state. Support for some of our research described in this review includes that from The National Science Council (Grants 89-2113-M-001-056, 90-2113-M-001-061, 91-2113-M-001-010, and 92-2113-M-001-064) and Academia Sinica.

References

(1) Tang, C. W.; VanSlyke, S. A. *Appl. Phys. Lett.* **1987**, *51*, 913.
(2) Tang, C. W.; VanSlyke, S. A.; Chen, C. H. *Appl. Phys. Lett.* **1989**, *65*, 3610.
(3) (a) Hung, L. S.; Chen, C. H. *Mater. Sci. Eng.* **2002**, *R39*, 143. (b) Fuhrmann, T.; Salbeck, J. *MRS Bull.* **2003**, *28* (*5*), 354.
(4) (a) Copper, A. D.; Cok, R. S.; Feldman, R. D. *Proc. SPIE − Int. Soc. Opt. Eng.* **2001**, *4105*, 18. (b) The standard red color for National Television System Committee (NTSC) is stricter with (0.67, 0.33) CIE color chromaticity coordinates.
(5) Kido, J.; Okamoto, Y. *Chem. Rev.* **2002**, *102*, 2357.
(6) (a) Adachi, C.; Baldo, M. A.; Forrest, S. R. *Appl. Phys. Lett.* **2000**, *87*, 8049. (b) Hong, Z.; Liang, C.; Li, R.; Li, W.; Zhao, D.; Fan, D.; Wang, D.; Chu, B.; Zang, F.; Hong, L.-S.; Lee, S.-T. *Adv. Mater.* **2001**, *13*, 1241. (c) Sun, P.-P.; Duan, J.-P.; Shih, H.-T.; Cheng, C.-H. *Appl. Phys. Lett.* **2002**, *81*, 792. (d) Liang, F.; Zhou, Q.; Cheng, Y.; Wang, L.; Ma, D.; Jing, X.; Wang, F. *Chem. Mater.* **2003**, *15*, 1935. (e) Sun, M.; Xin, H.; Wang, K.-Z.; Zhang, Y.-A.; Jin, L.-P.; Huang, C.-H. *Chem. Commun.* **2003**, 702. (f) Sun, P.-P.; Duan, J.-P.; Lih, J.-J.; Cheng, C.-H. *Adv. Funct. Mater.* **2003**, *13*, 683. (g) Fang, J.; Ma, D. *Appl. Phys. Lett.* **2003**, *83*, 4041.
(7) For iridium complex red emitters: (a) Adachi, C.; Baldo, M. A.; Forrest, S. R.; Lamanky, S.; Thompson, M. E.; Kwong, R. C. *Appl. Phys. Lett.* **2001**, *78*, 1622. (b) Lamansky, S.; Djurovich, P.; Murphy, D.; Abdel-Razzaq, F.; Lee, H.-E.; Adachi, C.; Burrows, P. E.; Forrest, S. R.; Thompson, M. E. *J. Am. Chem. Soc.* **2001**, *123*, 4304. (c) Duan, J.-P.; Sun, P.-P.; Cheng, C.-H. *Adv. Mater.* **2003**, *15*, 224. (d) Su, Y.-J.; Huang, H.-L.; Li, C.-L.; Chien, C.-H.; Tao, Y.-T.; Chou, P.-T.; Datta, S.; Liu, R.-S. *Adv. Mater.* **2003**, *15*, 884. (e) Tsuboyama, A.; Iwawaki, H.; Furugori, M.; Mukaide, T.; Kamatani, J.; Igawa, S.; Moriyama, T.; Miura, S.; Takiguchi, T.; Okada, S.; Hoshino, M.; Ueno, K. *J. Am. Chem. Soc.* **2003**, *125*, 12971. For platinum porphyrin complex red emitters: (f) Baldo, M. A.; O'Brien, D. F.; You, Y.; Shoustikov, A.; Sibley, S.; Thompson, M. E.; Forrest, S. R. *Nature* **1998**, *395*, 151. (g) O'Brien, D. F.; Baldo, M. A.; Thompson, M. E.; Forrest, S. R. *Appl. Phys. Lett.* **1999**, *74*, 442. (h) Kwong, R. C.; Sibley, S.; Dubovoy, T.; Baldo, M.; Forrest, S. R.; Thompson, M. E. *Chem. Mater.* **1999**, *11*, 3709. (i) Che, C.-M.; Hou, Y.-J.; Chan, M. C. W.; Guo, J.; Liu, Y.; Wang, Y. *J. Mater. Chem.* **2003**, *13*, 1362.
(8) Bulović, V.; Shoustikov, A.; Baldo, M. A.; Bose, E.; Kozlov, V. G.; Thompson, M. E.; Forrest, S. R. *Chem. Phys. Lett.* **1998**, *287*, 455.
(9) Kijimama, Y.; Nobutoshi, A.; Noriyuki, K.; Tamura, S.-i. *IEEE Trans. Electron. Devices* **1997**, *44*, 1222.
(10) Hamada, Y.; Kanno, H.; Tsujioka, T.; Takahashi, H.; Usuki, T. *Appl. Phys. Lett.* **1999**, *75*, 1682.
(11) Liu, T.-H.; Iou, C.-Y.; Wen, S.-W.; Chen, C.-H. *Thin Solid Films* **2003**, *441*, 223.
(12) Liu, T.-H.; Iou, C.-Y.; Chen, C. H. *Appl. Phys. Lett.* **2003**, *83*, 5241.
(13) Chen, C. H.; Tang, C. W.; Shi, J.; Klubek, K. P. *Thin Solid Films* **2000**, *363*, 327.
(14) (a) Popovic, Z.; Aziz, H. *Sel. Top. Quantum Electron.* **2002**, *80*, 874. (b) Young, R. H.; Tang, C. W.; Marchetti, A. P. *Appl. Phys. Lett.* **2002**, *80*, 874.
(15) Xie, Z. Y.; Hung, L. S.; Lee, S. T. *Appl. Phys. Lett.* **2001**, *79*, 1048.
(16) Feng, J.; Li, F.; Gao, W.; Cheng, G.; Xie, W.; Liu, S. *Appl. Phys. Lett.* **2002**, *81*, 2935.
(17) Chen, B.; Lin, X.; Cheng, L.; Lee. C.-s.; Gambling, W. A.; Lee, S.-t. *J. Phys. D*: *Appl. Phys.* **2001**, *23*, 30.
(18) Mitsuya, M.; Suzuki, T.; Koyama, T.; Shirai, H.; Taniguchi, Y.; Satsuki, M.; Suga, S. *Appl. Phys. Lett.* **2000**, *77*, 3272.
(19) Zhang, X. H.; Chen, B. J.; Lin, X. Q.; Wong, O. Y.; Lee, C. S.; Kwong, H. L.; Lee, S. T.; Wu, S. K. *Chem. Mater.* **2001**, *13*, 1565.
(20) Jung, B.-J.; Yoon, C.-B.; Shim, H.-K.; Do, L.-M.; Zyung, T. *Adv. Funct. Mater.* **2001**, *11*, 430.
(21) Ma, C.-Q.; Liang, Z.; Wang, X.-S.; Zhang, B.-W.; Cao, Y.; Wang, L.-D.; Qiu, Y. *Synth. Met.* **2003**, *138*, 537.

(22) (a) Tao, X. T.; Miyata, S.; Sasabe, H.; Zhang, G. J.; Wada, T.; Jiang, M. H. *Appl. Phys. Lett.* **2001**, *78*, 279. (b) Li, J.; Liu, D.; Hong, Z.; Tong, S.; Wang, P.; Ma, C.; Lengyel, O.; Lee, C.-S.; Kwong, H.-L.; Lee, S. *Chem. Mater.* **2003**, *15*, 1486.
(23) (a) Burrows, P. E.; Forrest, S. R.; Silbey, S. P.; Thompson, M. E. *Appl. Phys. Lett.* **1996**, *69*, 2959. (b) Shen, Z.; Burrows, P. E.; Bulović, V.; Forrest, S. R.; Thompson, M. E. *Science* **1997**, *276*, 2009.
(24) (a) Sakakibara, Y.; Okutsu, S.; Enokida, T.; Tani, T. *Thin Solid Films* **2000**, *363*, 29. (b) Sakakibara, Y.; Okutsu, S.; Enokida, T.; Tani, T. *Appl. Phys. Lett.* **1999**, *74*, 2587.
(25) Zhang, X. H.; Xie, Z. Y.; Wu, F. P.; Zhou, L. L.; Wong, O. Y.; Lee, C. S.; Kwong, H. L.; Lee, S. T.; Wu, S. K. *Chem. Phys. Lett.* **2003**, *382*, 561.
(26) Yu, J.; Shirota, Y. *Chem. Lett.* **2002**, 984.
(27) Wang, P.; Hong, Z.; Xie, Z.; Tong, S.; Wong, O.; Lee, C.-S.; Wong, N.; Hung, L.; Lee, S. *Chem. Commun.* **2003**, 1664.
(28) Mori, T.; Miyachi, K.; Kichimi, T.; Mizutani, T. *Jpn. J. Appl. Phys.* **1994**, *33*, 6594.
(29) Aminaka, E.-i.; Tsutsui, T.; Saito, S. *J. Appl. Phys.* **1996**, *79*, 8808.
(30) Zhang, B.; Zhao, W.; Cao, Y.; Wang, X.; Zhang, Z.; Jiang, X.; Xu, S. *Synth. Met.* **1997**, *91*, 237.
(31) (a) Picciolo, L. C.; Murata, H.; Kafafi, Z. H. *Appl. Phys. Lett.* **2001**, *78*, 2378. (b) Murata, H.; Kafafi, Z. H. *Proc. SPIE − Int. Soc. Opt. Eng.* **2001**, *4105*, 474.
(32) Mi, B. X.; Gao, Z. Q.; Liu, M. W.; Chan, K. Y.; Kwong, H. L.; Wong, N. B.; Lee, C. S.; Hung, L. S.; Lee, S. T. *J. Mater. Chem.* **2002**, *12*, 1307.
(33) Toguchi, S.; Morioka, Y.; Ishikawa, H.; Oda, A.; Hasegawa, E. *Synth. Met.* **2000**, *111−112*, 57.
(34) Huang, T.-H.; Lin, J. T.; Tao, Y. T.; Chuen, C.-H. *Chem. Mater.* **2003**, *15*, 4584.
(35) (a) Konne, B. E.; Loy, D. E.; Thompson, M. E. *Chem. Mater.* **1998**, *10*, 2235. (b) Shirota, Y. *J. Mater. Chem.* **2000**, *10*, 1. (c) Strohriegl, P.; Grazulevicius, J. V. *Adv. Mater.* **2002**, *14*, 1439. (d) Thelakkat, M. *Macromol. Mater. Eng.* **2002**, *287*, 442.
(36) Kim, D. U.; Paik, S. H.; Kim, S.-H.; Tsutsui, T. *Synth. Met.* **2001**, *123*, 43.
(37) Yeh, H.-C.; Yeh, S.-J.; Chen, C.-T. *Chem. Commun.* **2003**, 2632.
(38) Thomas, K. R. J.; Lin, J. T.; Velusamy, M.; Tao, Y.-T.; Chuen, C.-H. *Adv. Funct. Mater.* **2004**, *14*, 83.
(39) Balaganesan, B.; Wen, S.-W.; Chen. C. H. *Tetrahedron Lett.* **2003**, *44*, 145.
(40) Yu, J.; Chen, Z.; Sone, M.; Miyata, S.; Li, M.; Watababe, T. *Jpn. J. Appl. Phys.* **2001**, *40*, 3201.
(41) Thomas, K. R. J.; Lin, J. T.; Tao, Y.-T.; Chuen, C.-H. *Adv. Mater.* **2002**, *14*, 822.
(42) Wu, W.-C.; Yeh, H.-C.; Chan, L.-H.; Chen, C.-T. *Adv. Mater.* **2002**, *14*, 1072.
(43) Chiu, C.-W.; Chow, T. J.; Chuen, C.-H.; Lin, H.-Me.; Tao, Y.-T. *Chem. Mater.* **2003**, *15*, 4527.
(44) Seguy, I.; Jolinat, P.; Destruel, P.; Farence, J.; Mamy, R.; Bock, Ip, J.; Nguyen, T. P. *J. Appl. Phys.* **2001**, *89*, 5442.
(45) Lim, S.-T.; Chun, M. H.; Lee, K. W.; Shin, D.-D. *Opt. Mater.* **2002**, *21*, 217.
(46) Odom, S. A.; Parkin, S. R.; Anthony, J. E. *Org. Lett.* **2003**, *5*, 4245.
(47) Ma, C.; Zhang, B.; Liang, Z.; Xie, P.; Wang, X.; Zhang, B.; Cao, Y. Jiang, X.; Zhang, Z. *J. Mater. Chem.* **2002**, *12*, 1671.
(48) Kwong, R. C.; Sibley, S.; Dubovoy, T.; Baldo, M.; Forrest, S. R.; Thompson, M. E. *Chem. Mater.* **1999**, *11*, 3709.
(49) Yeh, C.-H.; Chan, L.-H.; Wu, W.-C.; Chen, C.-T. *J. Mater. Chem.* **2004**, *14*, 1293.
(50) Kijima, Y.; Asai, N.; Tamura, S. *Jpn. J. Appl. Phys. 1* **1999**, *38*, 5274.
(51) Baldo, M. A.; Lamansky, S.; Burrows, P. E.; Thompson, M. E.; Forrest, S. R. *Appl. Phys. Lett.* **1999**, *75*, 4.
(52) Kwon, R. C.; Nugent, M. R.; Michalski, L.; Ngo, T.; Rajan, K.; Tung, Y.-J.; Weaver, M. S.; Zhou, T. X.; Hack, M.; Thompson, M. E.; Forrest, S. R.; Brown, J. *Appl. Phys. Lett.* **2002**, *81*, 162.

CM049679M